ELSEVIER

Chemical Engineering Journal 76 (2000) 103–114

Chemical Engineering Journal

www.elsevier.com/locate/cej

Simulation and optimization on the regenerative thermal oxidation of volatile organic compounds

B.-S. Choi, J. Yi *

School of Chemical Engineering, Seoul National University, Seoul 151-742, South Korea

Received 15 May 1999; received in revised form 8 June 1999; accepted 25 June 1999

Abstract

Volatile organic compounds (VOCs) are involved in the generation of ozone via reaction with atmospheric NO_x in the atmosphere through a photochemical pathway. One of the popular treatment processes for VOCs is thermal oxidation, since it shows high destruction and removal efficiency (DRE). A regenerative thermal oxidizer (RTO) is commonly used because of its high heat exchange efficiency. The process uses ceramic beds to capture heat from gases exiting the combustion zone. Steady and unsteady flow field, distributions of temperature, pressure and compositions of flue gas inside an RTO were simulated by computational fluid dynamics (CFD). The DRE of VOCs and the pollutant concentrations of CO and NO emitted from the RTO are estimated by incorporating two-step incomplete combustion reaction of VOCs and Zeldovich's NO formation mechanism. The model system was the oxidation of benzene, toluene and xylene by the RTO, which was composed of three beds packed with ceramic beads to exchange heat. The height of the ceramic beds was varied and the effect of change of height was investigated in terms of DRE and pressure drop. The objective of the study was to simulate the performance of the RTO and optimize the height of ceramic beds. In a preliminary calculation, more than 95% of DRE is obtained when the premixed flow velocity of VOCs–air is less than about 3 m/s at the steady state at a constant fuel rate of 0.469 m/s under the given conditions. A weak recirculation zone above the center bed appeared and the intensity of recirculation decreases when no fuel is added in the normal direction. This region represents the putative site for the formation of NO, while most of the CO produced is converted to CO_2 in the recirculation zone. The results show that a level of 1.0% of VOCs is sufficient to provide energy for the oxidation when heat is exchanged through the ceramic bed. A ceramic bed of 0.2 m in height is sufficient to operate properly at these conditions and 5 s is recommended as the stream switching time. The importance of this simulation study is that the performance of RTO can be calculated at any operating conditions without the need for a pilot stage. In addition, the results can provide insight and practical responses involved in the design of an industrial RTO unit.

Keywords: Volatile organic compounds (VOC); Regenerative thermal oxidation (RTO); Computational fluid dynamics

1. Introduction

Volatile organic compounds (VOCs), which arise from industrial sources and automotive exhaust, are the most common pollutants emitted into the atmosphere. VOCs are organic compounds, which photochemically react with NO_x in the air to form ozone, the latter being a major component of smog [1]. Inadequate handling and disposal of these compounds have resulted in worldwide pollution of soil and groundwater by vapor sorption [2].

Thermal oxidation systems, also known as fume incinerators, are no longer simple flares or afterburners. Modern thermal oxidizers are designed to achieve 95–99% destruction and removal efficiency (DRE) of virtually all VOCs. These systems can be designed to handle capacities of 1000–500 000 cfm and VOC concentration ranges from 100 to 2000 ppm. Nominal residence times range from 0.5 to 1.0 s. Thermal oxidizers are available with thermal-energy recovery options to reduce operating costs [3].

Thermal oxidation systems involve the combustion of VOCs in the temperature range of 700–1000°C. The actual operating temperature is dependent on the type of furnace and pollutant concentration in the influent stream, as well as the desired DRE. Removal of VOCs, which are difficult to combust or which are present at low inlet concentrations, requires a high heat input (high fuel costs) and retention time in the combustion zone to meet the desired DRE value. A high DRE, also requires high temperature and long retention times in the combustion zone. Inlet concentrations in

* Corresponding author. Tel.:+82-2-880-7438; fax:+82-2-885-6670
E-mail address: jyiecerl@snu.ac.kr (J. Yi)

1385-8947/00/$ – see front matter
PII: S1385-8947(99)00118-7

excess of 25% of the lower explosive limit (LEL) are generally avoided by oxidizer manufacturers because of potential explosion hazards [3].

Operating temperatures near 1000°C are capable of producing elevated levels of nitrogen oxides (from nitrogen in the air), a secondary pollutant which may, in turn, require further treatment, such as selective catalytic reduction. Halogenated compounds in the inlet stream are converted to their acidic counterparts. The production of significant quantities of acidic compounds may require the use of expensive corrosion-resistant materials for construction and additional acid gas controls, such as scrubbing [3].

Two types of thermal-energy recovery systems are in common use: regenerative and recuperative. Both these systems use the heat derived from the exhaust stream to preheat the incoming gas stream prior to entering the combustion zone [1].

Regenerative systems use ceramic (or other dense and inert material) beds to capture heat from gases exiting the combustion zone. As the bed approaches the combustion-zone temperature, heat transfer becomes inefficient and the exhaust gas stream is then switched to a lower temperature bed. The incoming gas stream is then passed through the heated bed — where the captured heat is — prior to entering the combustion zone. The use of multiple beds permits regenerative systems to achieve up to 95% recovery of the thermal-energy input to the system as fuel and the heat content of the combusted VOCs. Whereas the incoming gas stream contains sufficient thermal-energy potential from VOC combustion, regenerative systems can operate without the need for an external fuel (excluding the need for a pilot light).

The efficiency of the thermal-recovery system depends on process-operating characteristics. A process where the flow rate and VOC content are relatively constant has good potential for achieving virtually no fuel operation. Cyclic processes generally are not entirely compatible with regenerative oxidation systems. The absorbed heat is lost to the environment during periods of low activity (that is, when air flow or VOC content is reduced). Operation with insufficient VOC content to supply thermal input requires the use of external fuel sources.

Recuperative thermal-oxidation systems recapture thermal energy with a simple metallic heat exchanger, typically a shell-and-tube design. The maximum thermal-energy recovery of a recuperative system is ≈70% of the fuel and VOC combustion energy input to the system.

The design of an oxidizer for the burning of VOCs is hampered by the lack of an accurate mathematical model for the process; as a results, some semi-empirical correlations are sometimes applied. The prediction of the flow field and temperature distribution in an oxidizer is in a more advanced stage of development and involves the use of computational fluid dynamics (CFD) analysis, although further validation data is still required.

The objective of this CFD study is to estimate the DRE of VOCs and the pollutant concentrations of CO and NO emitted from an incinerator which involves a two-step incomplete combustion reaction with Zeldovich's NO formation mechanism. The system studied involved the oxidation of three VOC components, benzene, toluene and xylene, by a regenerative thermal oxidizer (RTO), composed of three beds which are packed with ceramics for the heat exchanger.

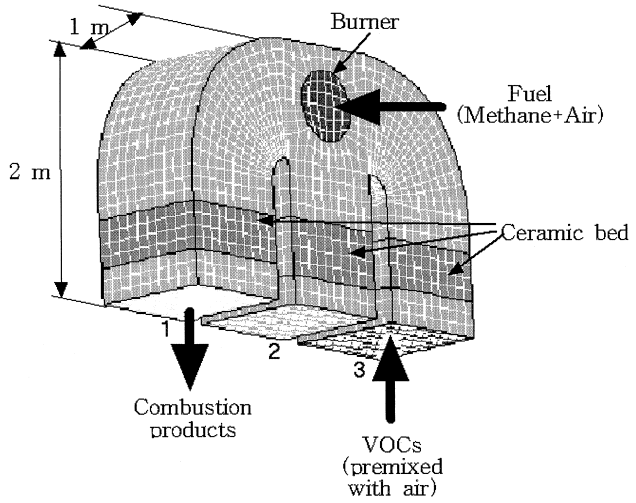

Fig. 1. Schematic description of three-bed regenerative thermal oxidizer (RTO) and grid for calculation.

The data has the potential for predicting fluid flow, temperature and oxidation products over total feasible and arbitrary operating conditions.

2. Characterization of the system

The schematic diagram of a typical three-bed regenerative thermal oxidizer (RTO), containing packed ceramic materials, is presented in Fig. 1. The dimension of the duct is $1\,m \times 1\,m \times 1\,m$ and height of the oxidizer 2 m. A burner, of diameter 0.6 m, is located at the center of a vertical wall in the normal direction. The grid employed is a body-fitted coordinate system and the number of grids is 14091 ($61 \times 21 \times 11$).

A three-bed RTO has the following functional mode: The VOCs–air premixture penetrates into the lower part of Section 3 of the bed in Fig. 1, where it is warmed on contact with hot ceramic packing which has been heated by the combustion gases of the previous cycle. At the exit of Bed 3, the mixture enters the combustion chamber, located above the three beds of the incinerator. A burner using CH_4 gas as the fuel maintains the temperature of the combustion chamber. The mixture of organic vapor and air is ignited and oxidized in this chamber to form CO, CO_2, NO and H_2O. The combustion gas then passes through Bed 1, where it is cooled through contact with the packing. The stored energy would then be used to preheat the incoming gases during the next cycle. While this cycle is running, the unused Bed 2 is purged with hot clean gases. This step is called the regen-

Table 1
Characteristics of the simulation cases

Case no.	Time scheme	VOCs inlet velocity (m/s)	Burner fuel velocity (m/s)	Flow direction	Height of bed (m)
A1	steady	0.00	0.469	Bed 3 → Bed 1	0.4
A2	steady	0.50	0.469	Bed 3 → Bed 1	0.4
A3	steady	2.00	0.469	Bed 3 → Bed 1	0.4
A4	steady	4.00	0.469	Bed 3 → Bed 1	0.4
A5	steady	10.00	0.469	Bed 3 → Bed 1	0.4
A6	steady	15.00	0.469	Bed 3 → Bed 1	0.4
B1	unsteady(0.5 s)	0.50	0	Bed 1 → Bed 3	0.4
B2	unsteady(1 s)	0.50	0	Bed 1 → Bed 3	0.4
B3	unsteady(10 s)	0.50	0	Bed 1 → Bed 3	0.4
B4	unsteady(60 s)	0.50	0	Bed 1 → Bed 3	0.4
B5	unsteady(120 s)	0.50	0	Bed 1 → Bed 3	0.4
B6	unsteady(180 s)	0.50	0	Bed 1 → Bed 3	0.4
B7	unsteady(300 s)	0.50	0	Bed 1 → Bed 3	0.4
B8	steady	0.50	0	Bed 1 → Bed 3	0.4
C1	unsteady(0–10 s)	0.50	0	Bed 1 → Bed 3	0.1
C2	unsteady(0–10 s)	0.50	0	Bed 1 → Bed 3	0.2

Table 2
The content of each compound set in the study and LEL of VOCs

VOC	Content of cases (vol %)	LEL (vol %)
Benzene	1.0	1.4
Toluene	1.0	1.3
Xylene	1.0	1.0

eration of ceramic bed. The role of this process is to purge any organic vapors or carbons in the bed remained from the previous cycle. This regeneration step is repeated to all three beds in turn.

The cases set in the study are listed in Table 1. A1–A6 are the steady-state cases for increasing velocity of the VOCs–air stream at constant fuel rate. The 0.469 m/s of fuel-air injection velocity corresponds to 2000 kJ per Nm^3/h of fumes. Fuel is continuously added into the oxidizer in all steady cases. In addition, unsteady scheme for changing the inlet duct is examined in cases B1–B8. The velocity of the VOCs–air stream is 0.50 m/s and no external fuel is added for all cases. Thus, the source of energy for oxidation is the regenerative heat in the ceramic bed. Concentrations of three VOCs — benzene, toluene and xylene — are 1.0 vol% in the air, respectively. It should be noted that this content is, in practice, very high although lower than the LEL of each component.

The effects of ceramic bed height on the DRE and pressure drop are investigated for the cases of C1 and C2. The heights of the ceramic bed are 0.1 and 0.2 m, respectively. The value of 0.4 m is set in all other cases as the height of the ceramic bed, except for cases of C1 and C2.

Table 2 lists the composition of the cases and LEL of each compound. As discussed earlier, all of the inlet compositions are lower than the LEL contents.

3. Mathematical modeling

The independent variables are the three components of the Cartesian coordinate system, (x,y,z) and time, t. The dependent variables are: the three velocity components, u, v and w in the x, y and z directions (m/s), respectively; the pressure P (N/m^2); the gas phase VOC concentrations, C ($kmol/m^3$); the gas phase temperature, T (K); and two characteristics of gas turbulence, namely the turbulence kinetic energy k (m^2/s^2), and its dissipation rate, ϵ (m^3/s^2).

The time-dependent equations for continuity, velocity components, temperature, chemical-species concentration and turbulence are given below.

Continuity:

$$\frac{\partial \rho}{\partial t} + \mathrm{div}\,(\rho u_i) = 0 \tag{1}$$

The pressure variable is associated with the continuity equation in anticipation of the so-called pressure-correction equation, SIMPLE(semi-implicit method for pressure-linked equation) [4], which is deduced from the finite-difference form of the equation of continuity. In the above equation, ρ represents the density and u_i, the velocity vector.

3.1. Momentum equations

In Cartesian coordinates, the unsteady-state equations of motion may be conveniently presented in the following form.

$$\frac{\partial}{\partial t}(\rho u_i) + \frac{\partial}{\partial x_j}(\rho u_i u_j) = \frac{\partial p}{\partial x_i} + \frac{\partial \tau_{ij}}{\partial x_j} + \rho g_i + F_i \tag{2}$$

Energy equation: An energy balance for the system with turbulence leads to the following equation.:

$$\frac{\partial}{\partial t}(\rho h) + \frac{\partial}{\partial x_i}(\rho u_i h) = \frac{\partial}{\partial x_i}\left[\left(\frac{\mu + \mu_t}{\delta_h}\right)\left(\frac{\partial h}{\partial x_i}\right)\right] + S_h \tag{3}$$

For a turbulent flow, the velocity consists of two components, one is the average velocity, $\bar{u}_i$ and the other the velocity fluctuation, u'_i.

$$u_i = \bar{u}_i + u'_i \tag{4}$$

Substituting Eq. (4) into the basic momentum balance, Eq. (2) yields the ensemble-averaged momentum equation. The equation has the same form as the fundamental momentum balance with velocities representing time-averaged values and the effect of turbulence incorporated through the 'Reynolds stresses', $\rho\overline{u'_i u'_j}$. The k–ε turbulence model is an eddy–viscosity model in which the Reynolds stresses are assumed to be proportional to the mean velocity gradients, with the constant of proportionality being the turbulent viscosity, μ_t. This assumption, known as the Boussinesq hypothesis, provides the following expression for the Reynolds stresses :

$$\rho\overline{u'_i u'_j} = \rho\frac{2}{3}k\delta_{ij} - \mu_t\left(\frac{\partial u_i}{\partial x_j} + \frac{\partial u_j}{\partial x_i}\right) + \frac{2}{3}\mu_t\frac{\partial u_i}{\partial x_i}\delta_{ij} \tag{5}$$

Table 3
Reaction mechanism

Function	Reaction mechanism	Ref.
Combustion of fuel	$CH_4 + 2\ O_2 \rightarrow CO_2 + 2H_2O$	[6]
Oxidation of benzene	$C_6H_6 + 9/2\ O_2 \rightarrow 6\ CO + 3\ H_2O$	[6]
Oxidation of toluene	$C_7H_8 + 11/2\ O_2 \rightarrow 7\ CO + 4\ H_2O$	[6]
Oxidation of xylene	$C_8H_{10} + 13/2\ O_2 \rightarrow 8\ CO + 5\ H_2O$	[6]
Reversible reaction between CO and CO_2	$CO + 1/2\ O_2 \leftrightarrow CO_2$	[9]
Formation of O radical	$O_2 \leftrightarrow O + O$	[10]
Zeldovich mechanism	$N_2 + O \leftrightarrow NO + N;\ N + O_2 \leftrightarrow NO + O$	[11]

Here, k represents the turbulent kinetic energy. The form of the Reynolds averaged momentum equations remain identical to the form of the laminar momentum equations, except that μ is replaced by an effective viscosity term, μ_{eff}:

$$\mu_{\text{eff}} = \mu + \mu_{\text{t}} \tag{6}$$

The turbulent viscosity μ_{t} is obtained by assuming that it is proportional to the product of a turbulent velocity scale and a length scale.

3.2. Turbulence model (k–ε model)

The value of k and ε are obtained by solving the conservation equations of turbulent energy:

$$\frac{\partial}{\partial t}(\rho k) + \frac{\partial}{\partial x_i}(\rho u_i k) = \frac{\partial}{\partial x_i}\left(\frac{\mu_t}{\sigma_k}\frac{\partial k}{\partial x_i}\right) + G_k + G_b - \rho\varepsilon \tag{7}$$

$$\frac{\partial}{\partial t}(\rho\varepsilon) + \frac{\partial}{\partial x_i}(\rho u_i \varepsilon) = \frac{\partial}{\partial x_i}\left(\frac{\mu_t}{\sigma_\varepsilon}\frac{\partial \varepsilon}{\partial x_i}\right) + C_1\frac{\varepsilon}{k}(G_k + (1 - C_3)G_b) - C_2\rho\frac{\varepsilon^2}{k} \tag{8}$$

where C_1, C_2, C_3, σ_{k} and σ_ε represent empirical constants, G_{k} the rate of production of turbulent kinetic energy and G_{b} the generation of turbulence due to the buoyancy.

3.3. Chemical reaction model

The VOCs are rapidly consumed during oxidation, forming as a result CO, NO and H_2O. The oxidation of CO to CO_2 proceeds somewhat more slowly. The difference in reaction rates can be taken into account using a two-step model, which is only slightly more complicated than the single-step model. It is capable of separating the relatively slow oxidation of CO to CO_2 from the more rapid oxidation of the VOCs to CO and H_2O [5], as,

$$C_nH_m + \left(\frac{n}{2} + \frac{m}{4}\right)O_2 \rightarrow nCO + \frac{m}{2}H_2O \tag{9}$$

$$CO + \tfrac{1}{2}O_2 \leftrightarrow CO_2 \tag{10}$$

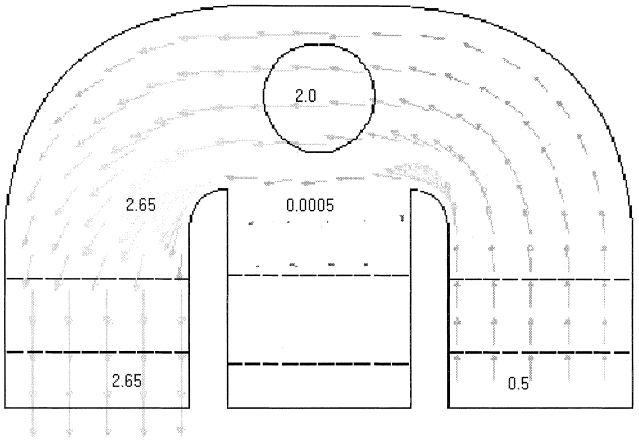

Fig. 2. Velocity vector and its two-dimensional magnitude in m/s for case A2

The reaction rate for Eq. (9) can be empirically expressed by

$$R = AT^n \exp\left[\frac{-E}{RT}\right][C_nH_m]^a[O_2]^b \tag{11}$$

Carbon monoxide oxidation of reaction, Eq. (10), can be described as:

$$R = AT^n \exp\left[\frac{-E}{RT}\right][H_2O]^c[O_2]^d[CO] \tag{12}$$

where the parameters for the oxidation of VOCs are taken from Westbrook and Dryer [6]. In the oxidation of CO, the dependence on the concentration of H_2O is included as shown in equation (12) and the reaction rate coefficients are estimated based on kinetic arguments. The concentration of H_2O in the rate expression implies that most of CO is consumed via the reaction with OH and the concentration of OH is assumed to be in equilibrium with water. [7].

The formation of NO via the oxidation of atmospheric nitrogen can be expressed in terms of the overall reaction, which is highly endothermic. As a result, the reaction of N_2 with O_2 is too slow to account for significant NO formation [7]. Free radicals, produced in flames via the dissociation of O_2, attack nitrogen molecules and begin a simple chain mechanism, which was first postulated by Zeldovich et al. [8], that is,

$$N_2 + O \leftrightarrow NO + N \tag{13}$$

$$N + O_2 \leftrightarrow NO + O \tag{14}$$

The reaction mechanism, called the Zeldovich mechanism, on NO formation was used in the reaction model for simplicity of analysis. It may result in underestimation of the NO level. The overall mechanisms which are assumed in this study are summarized in Table 3.

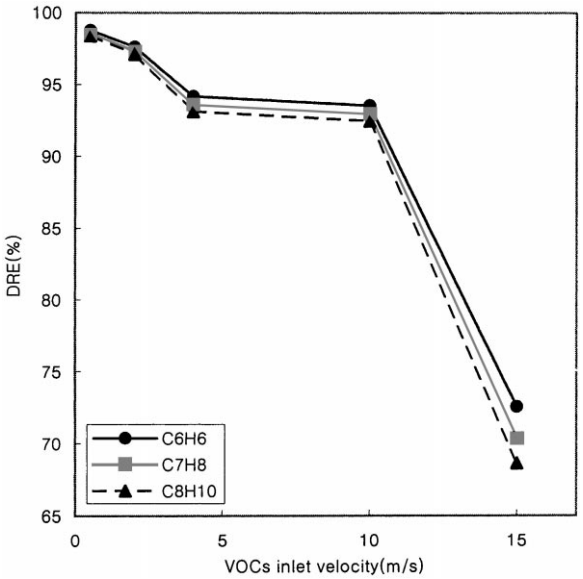

Fig. 3. Effect of inlet velocity of a VOC–air mixture on the destruction and removal efficiency (DRE).

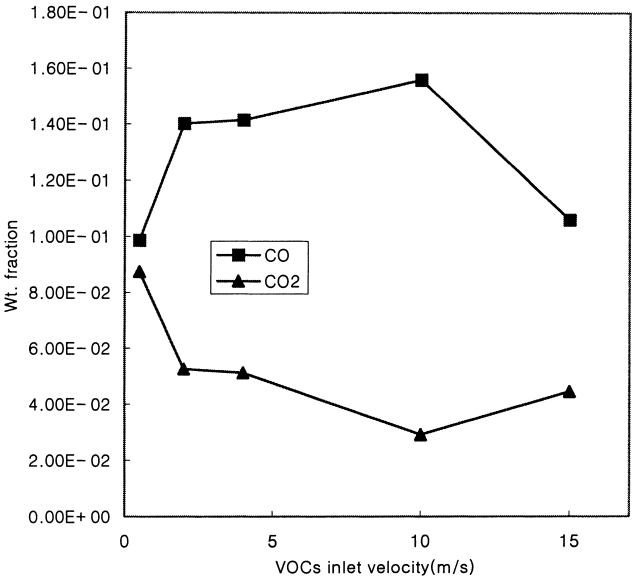

Fig. 5. Effect of inlet velocity of a VOC–air mixture on CO and CO_2 emission.

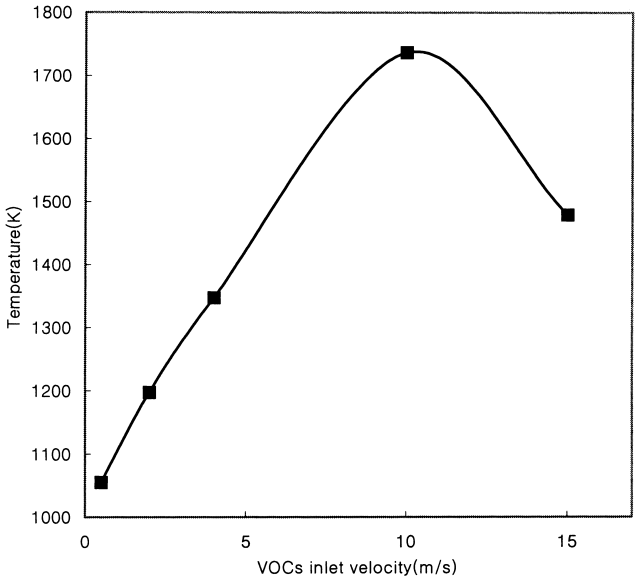

Fig. 4. Effect of inlet velocity of a VOC–air mixture on the temperature of combustion chamber.

4. Numerical calculations

A finite volume method (FVM), which combines features of the methods of Patankar [4] and a whole-field pressure-correction solver is utilized. The space dimensions (and time for transient cases) are discretized into finite intervals, and the variables are computed at only the finite number of locations at the grid points. These variables are connected with one another by algebraic equations (coupled finite-domain equations) derived from their differential counterparts by integration over the control volumes or cells, which are defined by the above intervals. An iterative procedure is used to solve the discretized differential equations. An alternate sweep direction within the marching plane was required to converge rapidly. Convergence was monitored by the variation between iterations of the field values of the dependent variables. When the magnitudes of residual sources fell below specified limits, convergence was assumed to have been achieved.

Adiabatic heat flux boundary conditions and a multi-grid simulation scheme for some variables were applied.

The calculations were performed on an SGI-OTHANE workstation running under UNIX. The FLUENT of version 4.4.7 was used as a solver.

5. Results and discussion

5.1. Estimation of RTO performance at steady-state conditions

The DRE of VOCs, the concentration of gas and energy use constitute three major criteria in evaluating the performance of an RTO. The distribution of fluid flow, temperature and concentration of exhaust gas over the range of feasible and arbitrary operating conditions can all be predicted without the necessity of a pilot test. First, the flow-field vectors for case A2 are shown in Fig. 2. The DRE of VOCs is strongly influenced by the velocity of the gas through the oxidizer. Peak velocities appear near the corner of the outlet duct. In the bed, the flow is evenly distributed in a normal direction. A weak recirculation zone, driven by the VOCs–air flow can be observed above the center bed. This is due to the typical geometry of the RTO and the location of ducts. The velocity increases rapidly in the region of the burner

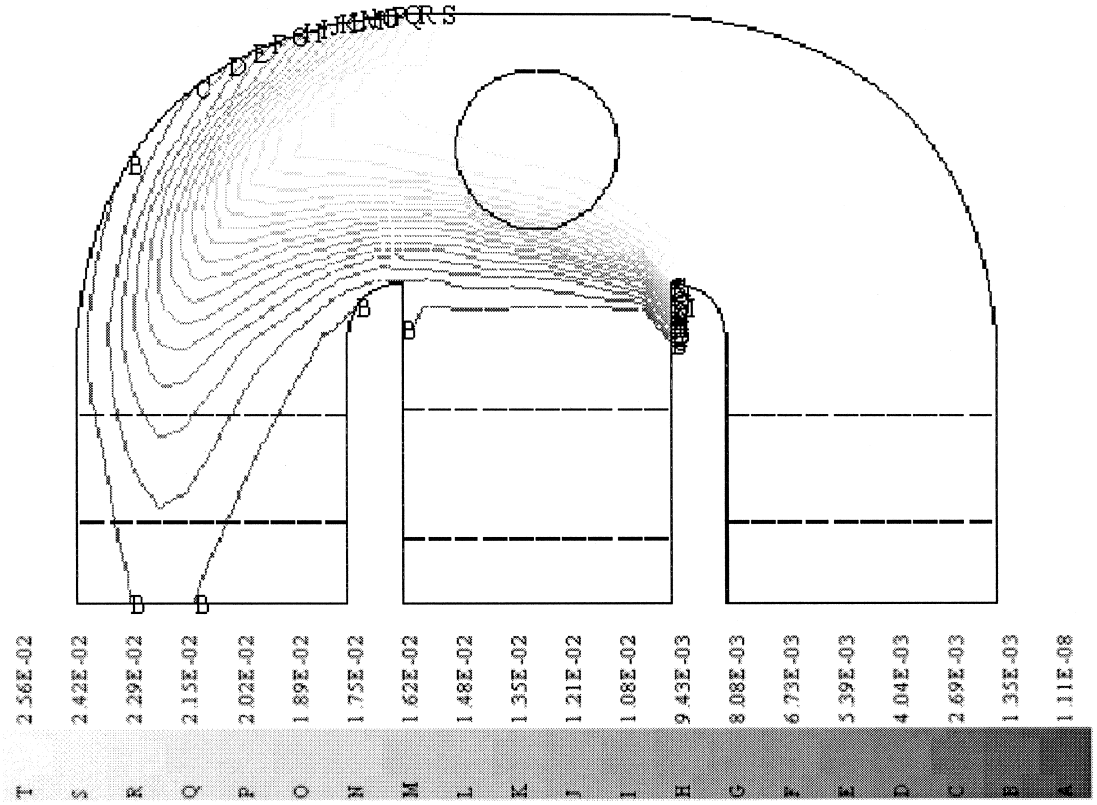

Fig. 6. Contour of C_6H_6 weight fraction for case A3.

and outlet duct because fuel is added to the system through the burner and the volumetric flow rate increases, as a result of the reaction and heat of oxidation. No apparent change in flow pattern can be detected for the cases of increasing VOCs–air velocity, except for an increase in the intensity of recirculation under the given conditions for cases A1 to A6.

The DRE of the VOCs is decreased with increasing inlet velocity of the VOCs–air mixture, as shown in Fig. 3. This is due to the reduction in residence time with increasing amounts of the inlet VOCs–air stream. The figure shows that >95% of DRE is obtained when the premixed flow velocity of VOCs–air is less than ≈3 m/s. The findings show that a velocity in excess of 10 m/s is too fast to properly treat the VOCs in this type of RTO. At an inlet stream velocity of 15 m/s, the DRE level decreases to 70%. This is related to temperature decrease. The results suggest that the maximal velocity to achieve the required DRE for other shapes of RTO could be examined without the need for a pilot stage study. Benzene, toluene and xylene show very similar trends in DRE reduction although they have different environmental effects and physical properties. This may be an advantage of thermal oxidation technology in the destruction of VOCs. This is due, largely, to the fact that DRE depends only on the kinetics of the oxidation reaction and that the kinetic parameters for these three compounds are similar. Of these three compounds, xylene is barely combustible, so it exhibits a relatively low DRE level.

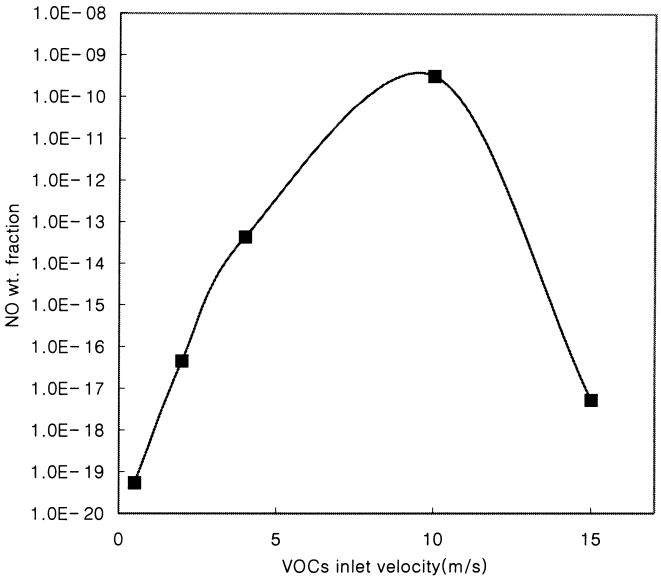

Fig. 7. Effect of inlet velocity of a VOC–air mixture on thermal NO emission.

Fig. 4 shows the temperature change of the combustion chamber with an increase in the rate of the VOCs–air flow rate to be treated. The temperature constantly increases with increasing, up to 10 m/s, VOCs velocity and decreases at the VOC mixture flow rate, 15 m/s. At this velocity, the temper-

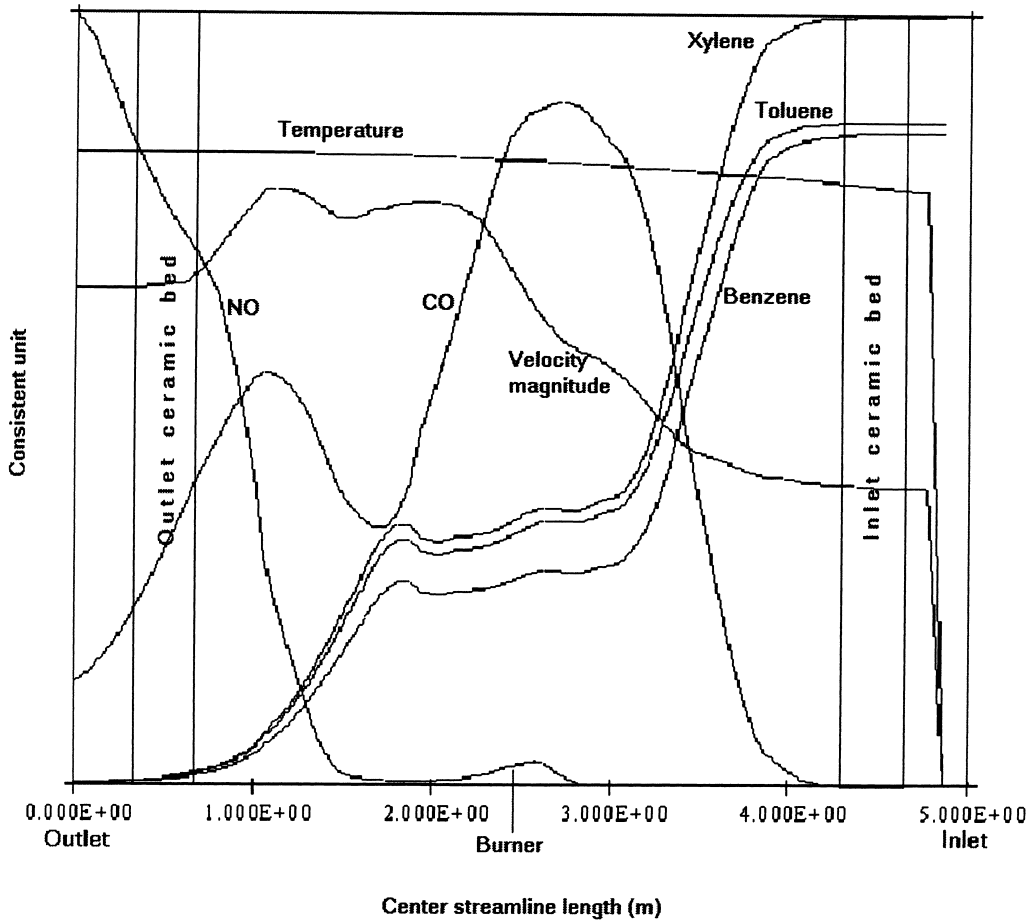

Fig. 8. Change of temperature, velocity magnitude and species concentration in the oxidizer along the central line from inlet to outlet (not to scale). Case A2.

ature and DRE decreases as shown in Fig. 3. It appears that this velocity is beyond the limit of the combustible range of fuel burning. The temperature increases up to 1736 K at 10 m/s of VOCs–air flow rate in this figure. In practice, an emergency control sequence is used in commercial RTOs to eliminate the risk of damage to the influent and discharge ducts and the interior of the equipment. A normal operating temperature range is in the range between 1000 and 1300 K. The result shows that the velocity of a VOCs–air stream below 5 m/s is recommended in this type of RTO.

Fig. 5 illustrates the effect of VOCs–air velocity on the concentration of CO and CO_2 emissions. The CO fraction increases with VOCs–air velocity while the CO_2 fraction decreases. These data suggest that complete combustion of the organic compounds is not achieved in this RTO. The results show that an increase in VOCs–air velocity, and a reduction in DRE level, cause incomplete combustion. Fig. 6 shows the contour of the mole fraction of benzene for case A3. A similar behavior is observed for other VOCs combustion. The VOC concentrations decrease along the stream and a rapid decrease is accomplished in the burning region. A relatively high level of contour appears in the region below the burner due to convective buoyancy forces. This result could be used to determine the setting position of the burner. The contour of the CO fraction shows a behavior similar to that in Fig. 6, except for a low CO concentration at the inlet region and a high CO concentration at outlet. A high concentration of CO_2 is observed in the recirculation zone, which suggests that a long retention time facilitates complete reaction of CO with O_2.

Fig. 7 shows that thermal NO emission increases with temperature, as expected. It is clear that the plot of amount of NO emission is very similar to that of the chamber temperature (Fig. 3). However, the level of NO may be underestimated, since the effect of OH radical on the formation of NO is omitted in this reaction model. The spatial distribution of NO contour shows a similar trend to CO_2 behavior though it is not depicted in this paper. A large portion of the NO emission is formed at the zone of flow recirculation. It should be noted that rapid CO_2 and NO formation reactions are observed in the recirculation zone as described above. This suggests that the proper retention time in the flame zone is an important factor in the design of an RTO with respect to baffle or shape without flow recirculation.

Fig. 8 shows useful information relative to spatial data for seven dependent variables along the centerline in the RTO.

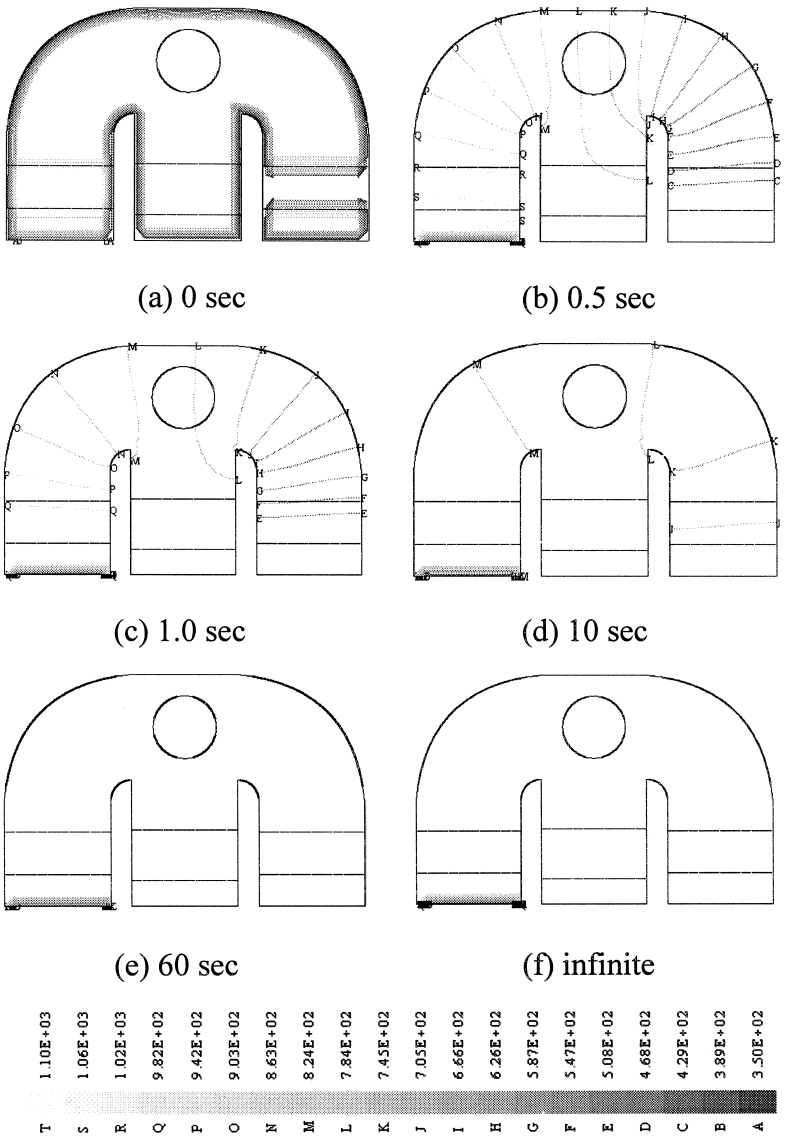

Fig. 9. Temperature (K) contours in the RTO as a function of time.

The trend of the each variable is shown. The length of the centerline reaches to ca 5.0 m with the right-hand side as the inlet and the left-hand side as the outlet of the RTO, as shown in Fig. 1. The location of center of the ceramic Bed 1 and of Bed 3 is at 0.5 and 4.5 m, respectively, and the burner is at 2.5 m in Fig. 8. The thickness of bed is 0.4 m. The magnitude of each variable is not scaled in this figure, since seven variables are included in one plot and the orders of these values are different. The steady-state temperature is constant over the entire range, except for the region under the inlet bed, since the VOCs–air stream starts to oxidize from the inlet ceramic bed, producing the heat of oxidation. The content of the VOCs decreases continuously and the rapid destruction and removal of these compounds occurs in the region of burning near the burner. Xylene shows a relative higher concentration level due to its kinetics parameters of oxidation. CO concentration reaches a maximum value at the center of the burning region, which is due to the reaction mechanism for the formation of CO in the first stage of oxidation, as expected. As mentioned earlier, a two-step scheme of incomplete oxidation is used in this study. The CO fraction decreases with increasing retention time. To the best of our knowledge, the distribution between CO and CO_2 depends on the time scale of mixing and reaction. The spatial profile of thermal NO is not similar to that of temperature in this figure. NO concentration constantly increases from burner to outlet, since the characteristic time of reaction for NO formation is longer than the residence time of gas flow. Thus, the profile of NO shows a gradual increase as it approaches the outlet, while the temperature is constant. The magnitude of the flow gas velocity is also included in Fig. 8. It increases after the addition of the fuel stream in a normal direction. The figure shows that CO level decreases abruptly after the burner region. This is the result of the increase in

intensity of mixing and the fact that added heat improves the extent of oxidation reaction in that region.

This type of spatial plot of some variables would be helpful with respect to the modification of the design of an RTO.

5.2. Unsteady-state simulation

The VOCs–air gas mixture is then fed into the lower part of Bed 1 in Fig. 1, which was the outlet of the earlier steady-state simulation. The inlet gas is preheated by contact with hot ceramic packing which was heated during the previous operation. The unsteady-state scheme is studied in cases of B1–B8 in Table 1. The velocity of the VOCs–air stream is set to 0.50 m/s, where 98.5% of average DRE was achieved in the steady-state operation. No external fuel is added in the cases of B1–B8 and, thus, the source of energy for oxidation is exclusively the regenerative heat in the ceramic bed.

The time-dependent temperature field in the RTO is shown in Fig. 9. It is assumed that the inlet ceramic bed (No. 1 in Fig. 1) has an initial temperature of 1050 K, because it was maintained at this temperature during the previous steady-state case, A2. The temperature of the outlet ceramic bed (No. 3 in Fig. 1) is set to 400 K. The initial distribution of temperature is included in Fig. 9. As shown in the figure, the computational fluid dynamics model of RTO provides an estimation of contour maps of temperature distribution with operating time. After 60 s, the temperature distribution approaches the result of the infinite case, although a small increase is detected. About 300 s are required to reach the steady state under the given conditions. The plot of flue-gas temperature for the unsteady cases, B1–B8, is shown in Fig. 10. The temperature increases rapidly up to 866 K at 180 s as the operating time increases, and it is then maintained at this temperature. More than 95% of the DREs of VOCs are obtained in all cases of B1–B8. It can thus be concluded that the heat of oxidation itself is sufficient to provide an energy source for combustion without the need for added fuel. This is mainly due to the high content of VOCs in air.

The steady-state cases provide similar velocity vectors to the unsteady cases, except for an increase in the intensity of the recirculation zone above the central bed. The reason for this is that the fuel/air flow is not added in a normal direction. Thus, burning a fuel through the burner not only provides heat for VOC combustion but also supplies energy for breaking the recirculation which appears in the central region.

Fig. 11 illustrates the contours of CO fraction as time progresses. The CO level increases along the flue gas reaching a maximum value at the right upper region above the outlet. A transient distribution of the CO fraction is found until it reaches 10 s and the distribution becomes similar after 60 s. Time-dependent contour propagation of VOCs concentration is very similar to the CO fraction, since the reaction mechanisms are formulated in a way that CO is generated directly by decomposition of VOCs in the simulation. Fig. 12 shows the fractions of CO and CO_2 emissions. CO and CO_2 fractions increase with the propagation of operating time and remain constant after 300 s. The ratio of CO to CO_2 reaches about 4.5.

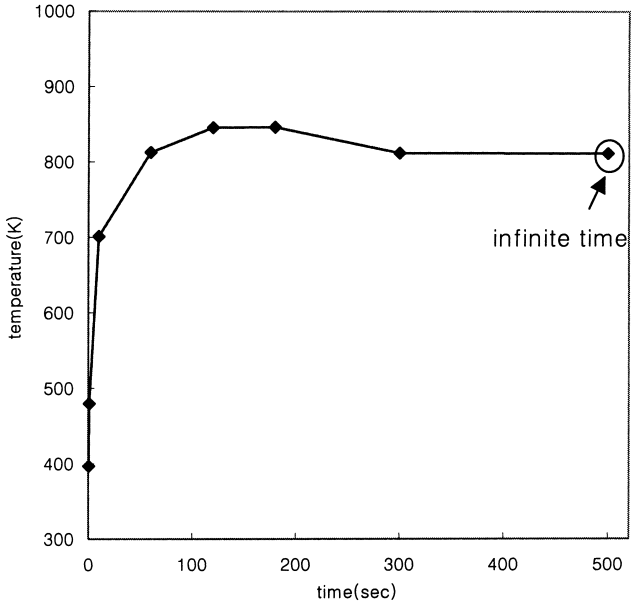

Fig. 10. Effluent temperature profile for the unsteady simulation.

The contours of CO_2 and NO show a similar pattern for spatial distribution as the operating time increases. The maximum values of both these fractions appear in the central region, below the burner. This region is identical with the flow recirculation zone. The long retention time for oxidative products with O_2 enhances the completeness of the oxidation reaction as described above. It should be noted that the amount of generated NO is very small, since the chamber temperature is <1000 K in the unsteady cases. Problems caused by NO emission may not be considerable at this operating condition without added fuel, because the probability of thermally generating NO is small at this low temperature.

In conclusion, the steady state is reached after 300 s in the view of changes in all the variables. Operating conditions for the 0.5 m/s of VOCs–air stream and 1.0% levels of each VOC perform properly when the heat exchanged equals 1050 K of the regenerative ceramic bed without added fuel.

5.3. Optimization of the height of the ceramic bed

The regenerative systems use ceramic beds to capture the heat from gases exiting the combustion zone. As the bed approaches the combustion zone temperature, heat transfer becomes inefficient and the combustion-exhaust gas stream is switched to a lower temperature bed. By using multiple beds, regenerative systems achieve a high recovery of the thermal-energy input to the system as fuel and the heat content of the combusted VOCs. Where the incoming gas stream contains sufficient thermal energy potential from VOC com-

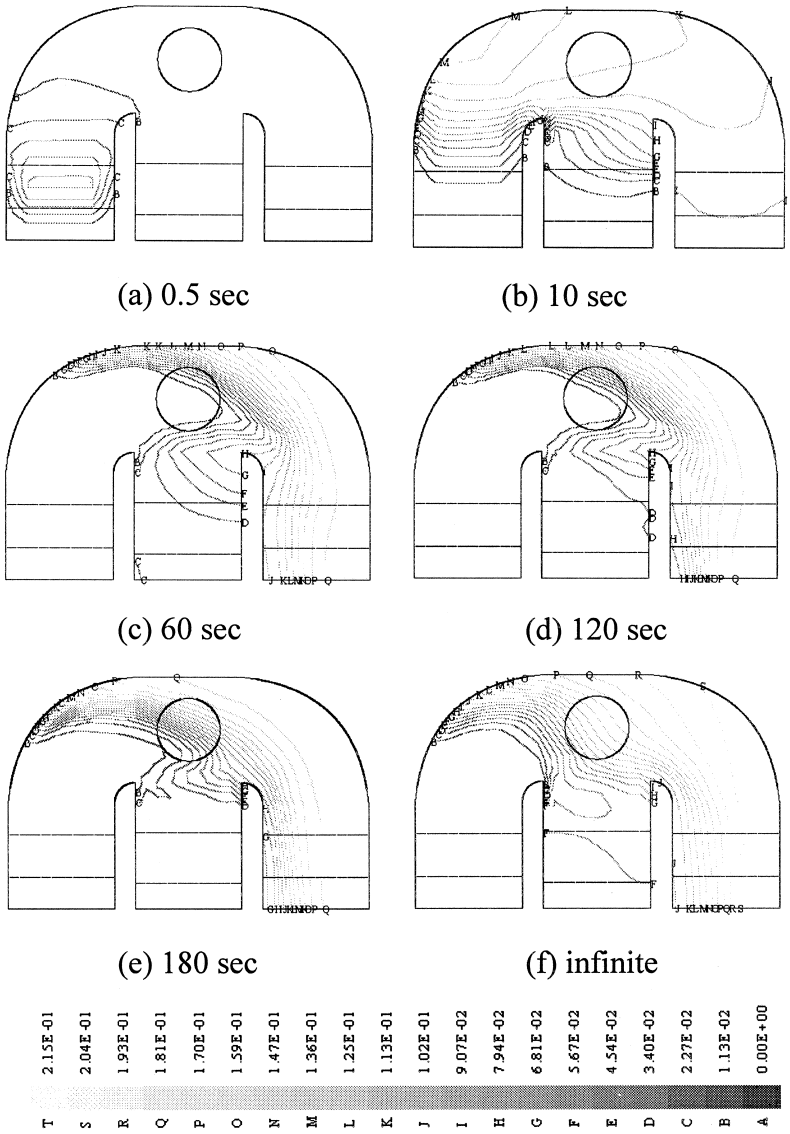

Fig. 11. Contours of the CO weight fraction in the RTO as a function of time.

bustion, regenerative systems can operate without the need for external fuel. A high ceramic bed is usually a preferred design for providing sufficient contact time to exchange the heat. This situation leads to high thermal recovery and desirable DRE of VOCs. However, it may cause a high pressure drop due to the momentum sink by the porous ceramic bed. Pressure drop is generally related to loss of power in an RTO operation, and so it should be minimized.

The effects of the height of the ceramic bed on the DRE and pressure drop were investigated in this study. The height of the ceramic bed varies as 0.1, 0.2 and 0.4 m in the cases of C1, C2 and all other cases, respectively. The velocity of the VOCs–air premixed stream is 0.5 m/s and auxiliary fuel is not supplied to the RTO, because the stream has a sufficient content of VOCs. In addition, the proper switching time of stream is found from the results of the simulation.

The DRE of VOCs is decreased with increasing time, regardless of the height of ceramic bed, as shown in Fig. 13. This is due to the reduction in the heat recovery factor as time increases. The DRE decreases more rapidly with increase of time when the height of the ceramic bed becomes lower. After 7 s, the DRE apparently decreases below 85% in the case of 0.1 m of height of bed. However, no significant differences between the results of 0.2 and 0.4 m high ceramic bed before 7 s were observed. More than 95% of the DRE is obtained prior to the time reaching 3, 5 and 7 s in the case of 0.1, 0.2 and 0.4 m of height of ceramic bed, respectively. Thus, the appropriate switching time for each case is 3, 5 and 7 s based on the 95% of DRE. These results suggest that a higher ceramic bed is advantageous in terms of effective heat exchange.

The result of pressure drop as a function of the height of the ceramic bed is shown in Fig. 14. The pressure drop increases as the height of bed increases. This drop is 1700 Pa in the case of 0.4 m high bed, which is about twice the value for 0.2 m and sixfold that of the 0.1 m high bed.

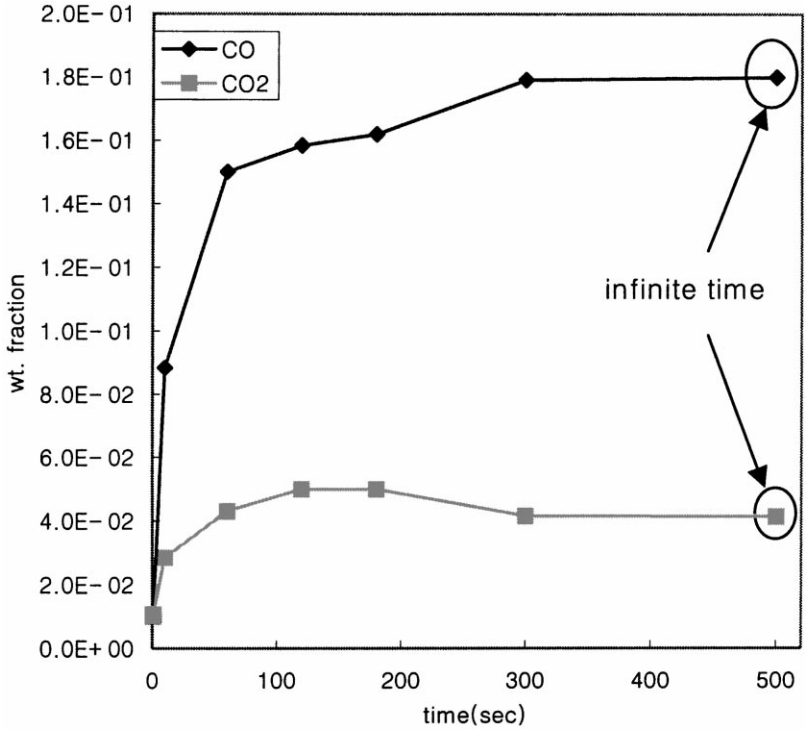

Fig. 12. Profiles of CO and CO_2 emission for the unsteady simulation.

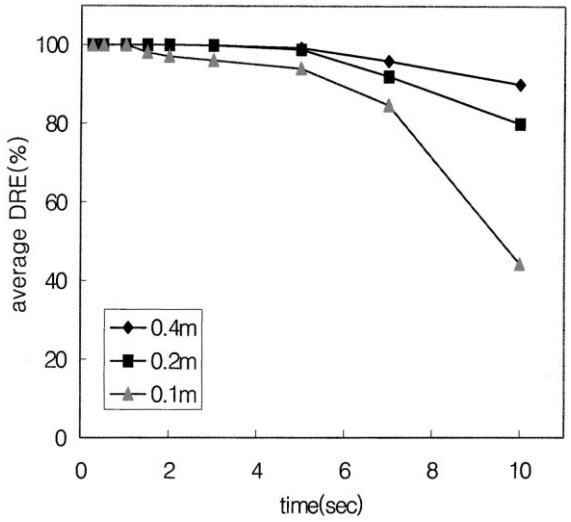

Fig. 13. Effect of height of ceramic bed on the average DRE of VOCs in unsteady simulation.

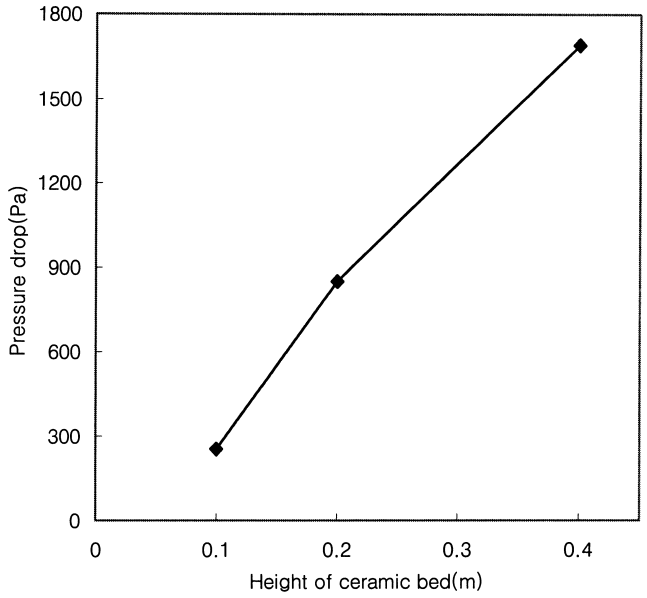

Fig. 14. The effect of height of ceramic bed on pressure drop.

It is concluded in the simulation that a 0.2-m high bed is the optimal choice to recover the thermal energy, minimize pressure drop and satisfy 95% of DRE when the stream switching time is 5 s.

6. Conclusions

A computational fluid dynamics (CFD) technique is developed and used to predict flow-field, temperature and concentration distribution of combustion emissions and unburned VOCs in a three-bed regenerative thermal oxidizer. Sample VOCs used in the cases are typical aromatic compounds, namely benzene, toluene and xylene. The importance of the proposed simulation results is that RTO performance can be calculated at arbitrary operating conditions and can provide insight and practical responses involved in the design of an industrial unit.

It is concluded that this approach can be properly applicable to testing arbitrary operating conditions, such as high level of VOCs and fast velocity of VOCs–air stream. Transient behavior of flow, temperature and concentration of each compound is also estimated as propagation of the operating time in the unsteady calculations. The data show that a 0.2-m high bed is the proper design from the point of view of thermal recovery, pressure drop and DRE. The recommended stream switching time is 5 s.

More quantitative analysis is required to validate the kinetic model estimating NO and other toxic combustion emissions after the comprehensive knowledge of reaction network and corresponding reaction rate coefficients. This study will be then extended to regenerative catalytic oxidation systems with the validation of the catalytic kinetic scheme.

7. Nomenclature

A	Arrhenius pre-exponential coefficient
C_1, C_2, C_3	turbulent empirical constants
C_6H_6	benzene
C_7H_8	toluene
C_8H_{10}	xylene
C_A	molar concentration of compound A
C_B	molar concentration of compound B
C_p	heat capacity
E_a	activation energy
F_i	external force
G_b	generation of turbulence due to buoyancy
G_k	generation of turbulent kinetic energy
g_i	gravity force
h	enthalpy
k	turbulent kinetic energy
p	pressure
R	gas-law constant
R'	reaction rate
S_h	generation term of enthalpy
t	time
μ_i	velocity component of *i*- direction
$\overline{u_i}$	time averaged velocity component of *i*-direction
u_i'	velocity fluctuation component of i-direction
x_i	Cartesian coordinate of *i*-direction
δ_h	turbulent Prandtl number for enthalpy
δ_{ij}	Kronecker delta
ε	dissipation rate of turbulent energy
μ	laminar viscosity
μ_{eff}	effective viscosity
μ_t	turbulent viscosity
ρ	density of fluid
σ_k	Prandtl number for turbulent energy
σ_ε	Prandtl number for dissipation rate
τ_{ij}	shear stress

References

[1] M.S. Jennings, N.E. Krohn, R.S. Berry, M.A. Palazzolo, R.M. Parks, K.K. Fidler, Catalytic incineration for control of volatile organic compound emissions. Radian Corp., Research Triangle Park, NC, 1985.
[2] T.G. Poulsen, P. Moldrup, T. Yamaguchi, J.W. Massmann, J.A. Hansen, J. Env. Eng. 124 (1998) 145.
[3] E.N. Ruddy, L.A. Carroll, Chem. Eng. Prog., July 89 (1993) 28.
[4] S.V. Patankar, Numerical Heat Transfer and Fluid Flow. McGraw–Hill, New York, 1980.
[5] D.J. Hautman, F.L. Dryer, K.P. Schug, I. Glassman, Combust. Sci. Tech. 25 (1981) 219.
[6] C.K. Westbrook, F.L. Dryer, Combust. Sci. Tech. 27 (1981) 31.
[7] R.C. Flagan, J.H. Seinfeld, Fundamentals of Air Pollution Engineering. Prentice Hall, NJ, 1988.
[8] Y.B. Zeldovich, P.Y. Sadovnikov, D.A. Frank-Kamenetskii, Oxidation of Nitrogen in Combustion, Academy of Science of USSR, Institute of Chemical Physics, Moscow–Leningrad, 1947 (M. Shelef, Trans.)